

## Research Article

# Anti-Overturning Bearing Capacity of Rigid and Flexible Concrete Expanded Piles Subjected to Horizontal Load

Yongmei Qian, Tingting Zhou, and Wei Tian 

Jilin Jianzhu University, Changchun 130118, China

Correspondence should be addressed to Wei Tian; 55356045@qq.com

Received 14 October 2019; Revised 20 April 2020; Accepted 26 May 2020; Published 8 July 2020

Academic Editor: Rosario Montuori

Copyright © 2020 Yongmei Qian et al. This is an open access article distributed under the Creative Commons Attribution License, which permits unrestricted use, distribution, and reproduction in any medium, provided the original work is properly cited.

The concrete expanded pile is a new type of pile in the field of foundation engineering, which exhibits improved performance compared to the ordinary straight-hole pile. The expanded technique increases the bearing capacity of the pile, changes the overall load-bearing function of the pile body, and offers great development prospects. While the performance of the expanded pile has been studied for vertical loading, the performance of expanded pile when subjected to horizontal loading is not adequately understood. In order to investigate the performance of concrete expanded pile in resisting horizontal loads, particularly the anti-overturning capacity of rigid and flexible piles, this paper conducts an experimental model test and performs a numerical simulation. In the experiment, an innovative model test method is used for testing small-scale half-face pile with undisturbed soil. A custom-made soil extractor and a loading device are used to observe various stages of pile-soil interaction in real-time during the whole process of loading. Meanwhile, finite element simulation analysis is conducted on a pile model and the corresponding data on displacement, load, stress, and strain are collected to verify the experimental results. Based on the horizontal bearing capacity of rigid and flexible piles and the failure states of soil mass around the piles, two calculation models are proposed for the horizontal bearing capacity of rigid and flexible concrete expanded piles. The models will provide reliable theoretical guidance for the application of concrete expanded pile in engineering applications and for the research and development of pile foundation.

## 1. Introduction

*1.1. Development Status of Concrete Expanded Pile.* In the past, bearing capacity of pile foundation was improved either by increasing the contact area between pile and soil through an increase in the pile length or by improving the pile tip resistance through an increase in the contact area of pile tip, or by a combination of both. However, an increase in the length of the pile involves more materials for construction and an increased cost of construction [1]. Moreover, due to an increase in the slenderness ratio, the compressive resistance of long piles is markedly reduced. As an improvement in engineering construction, variable-section piles are being increasingly used recently, thus promoting the development of cast-in-place pile.

Variable-section piles first appeared around the 1950s when Britain, India, the Soviet Union, and other countries began to drill multisection expanded pile in soft soil layers to

bear the load [2]. While piling technology started relatively late in China, it developed rapidly, and various pile types and construction methods were practiced. The development of variable-section piles in China began in the late 1970s. Even though variable-section piling has been applied globally, its technology is relatively new and few studies exist in this field. A promoting development in variable-section piling happened in China; namely, Beijing Building Mechanization Research Institute first developed a hole expander with three functions of extruding-expanding, drilling-expanding, and soil cleaning [3]. In 1998, Dexin summarized the development experience of pile foundation in China and abroad and proposed a patented technology—extruded-expanded branch cast-in-place pile, called “DX pile” for short [4]. DX piling adopts the biomimetic principle, studies the root shape and growth characteristics, combines its knowledge with the construction method applied in the project, and pours concrete through a hydraulic squeeze and expansion

device [5]. DX piling has become popular as a new practical pile foundation technology. As a further development of the technology, Baocheng from Beijing Rongchuang Geotechnical Engineering Co., Ltd., invented drilling-expanding machines and tools, such as “drilling, expanding, and cleaning all-in-one machine,” as shown in Figure 1, which greatly facilitated the construction of variable-section piles.

Concrete expanded pile (as shown in Figure 2) is a new type of expanded pile made by extruding-expanding, spinning-expanding, or drilling-expanding. It has stronger bearing and anti-overturning capacity and an excellent antisettlement performance, which has a wide range of applications [6]. The bearing expanding plate can be flexibly changed according to the field condition while bearing force, so as to shorten the pile length, saves the construction materials and shortens the construction time simultaneously. The concrete expanded pile is a new type of pile foundation, which is economical and practical and has better performance. According to the previous preliminary experimental study, it is found that the failure state of rigid and flexible piles under horizontal load is quite different, and the failure mechanism and the calculation method of bearing capacity should be determined separately. Many researchers do not recognize the problem, so there is no research on it. Scholars have conducted preliminary theoretical research and experimental research on concrete expanded pile under the action of horizontal load, basically investigating the effects of various parameters of load-bearing expanded plate such as plate location, plate gap, and plate diameter on the failure mode of the rigid expanded pile and determining the horizontal ultimate bearing capacity [7]. However, few studies exist on the ultimate bearing capacity of flexible expanded piles and soil damage around the piles under horizontal load. Therefore, this paper proposes a numerical model of horizontal anti-overturning bearing capacity of rigid and flexible piles by conducting a unique model test of small-scale half-face pile and performing an ANSYS finite element simulation. This model is expected to provide a theoretical basis for the design and development of concrete expanded pile. (Rigid pile refers to the large stiffness; under the action of horizontal load, the pile does not bend, but the overall overturning. Flexible pile means that the stiffness is not large; under the action of horizontal load, the pile is bent, and the whole overturning does not occur directly.)

*1.2. Research Contents and Innovation Points.* In this paper, model piles with rigid and flexible properties were taken as the research objects. Through an ANSYS finite element numerical simulation analysis and a test of the small-scale half-section model pile, the effects of soil failure states of rigid and flexible concrete expanded pile under horizontal load were studied, and then a calculation method for the anti-overturning capacity under horizontal load was determined. This paper has the following innovation points:

- (1) The simulation test involved innovative small-scale half-section model tests. Based on the loading device in the original vertical loading test, the testing device was improved to achieve simultaneous vertical and

horizontal loading. Comprehensively considering the model dimension and boundary effect, a special soil collector was designed, and the half-face pile was substituted for the whole pile to conduct the test design, so as to observe the soil damage phenomenon in the whole process of the test.

- (2) In order to better analyze the failure state of soil around the pile, ANSYS simulation analysis was performed corresponding to the model test to further confirm the reliability of the pile and soil failure mechanism.
- (3) According to the failure states of different piles, calculation models were proposed for different anti-overturning bearing capacities of rigid and flexible concrete expanded piles.

## 2. Experimental Study

In engineering practice, a pile foundation should possess high horizontal bearing capacity while bearing a relatively large vertical load. At present, research on concrete expanded pile under horizontal load is relatively limited. Since many factors remain uncertain in the process of a real pile test, and their prediction requires a long test period, the accuracy and timeliness of the structure cannot be guaranteed [8]. In this regard, a small-scale half-section model test scheme proposed by professor Yongmei was adopted in this paper. The test mainly involved test specimens and loading devices, which were processed and developed in a factory and were independently designed. An original soil collecting device was used mainly to provide undisturbed soil for the small-scale half-section model test. This ensured that the pile body worked essentially in the actual soil mass, the accuracy of test results was improved, and any changes in soil mass during the test could be observed so that the interaction between pile and soil could be observed [9]. This test method adopted in the model test provided a reliable experimental basis for the experimental study on the failure of soil around a concrete expanded pile.

*2.1. Model Pile Specimens.* This experimental study involved two groups of four specimens, and the positions of the plates in the two groups were different, namely, G3 and R3, and G4 and R4 as shown in Figure 3. In each group, G3 and G4 were rigid, R3 and R4 were flexible, and the distance between the bearing plate position of the model pile and the pile top was 40 mm and 160 mm, respectively. The pile length was  $L = 227$  (mm), the pile diameter was  $d = 16$  (mm), the plate diameter was  $D = 50$  (mm), the plate height was  $H = 27$  (mm), the plate slope angle was  $\alpha = 39^\circ$ , the overhanging length was  $R = 17$  (mm), and the distance between the plate and pile top was  $L_1 = 40$  (mm). The actual model pile is shown in Figure 3.

*2.2. Design of Soil Collector.* Q235 steel with high rigidity was selected as the material for soil collector, as shown in Figure 4. The size of the soil collector was 300 mm × 250 mm × 300 mm,



FIGURE 1: Expanding device of drilling, expanding, and cleaning all-in-one machine.

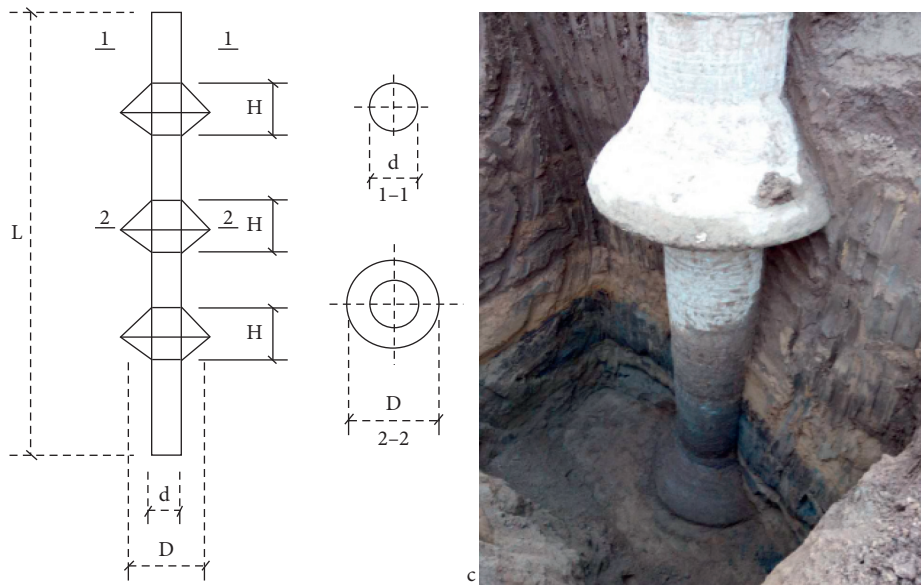


FIGURE 2: Schematic diagram for concrete expanded pile and a photograph of a real pile.

the plate thickness was 5 mm, and a relatively thick plate was used mainly to prevent the deformation of the soil collector in the actual site. The soil collector was provided with a removable function designed to install observable tempered glass.

A limit clamp and a fixed clamp were used in the test to fix the tempered glass and to prevent the disturbance of the soil collector itself in the experiment process.

2.3. Design of Test Rig. The loading device used in this test was an innovative multifunction loading rig, as shown in Figure 5. The loading device involved the design of a vertical loading device and a horizontal loading device, as shown in Figures 6 and 7.

In order to simulate the actual project, small-scale half-section model piles were designed to bear not only the



FIGURE 3: Model of rigid and flexible concrete expanded pile.

horizontal load but also the vertical load. The vertical loading device was made up of cystosepiment, shim, jack, load-bearing steel plate, and screw, as shown in Figure 5. In the test, a vertical load was applied through a jack and was transferred through a load-bearing plate. The horizontal loading device was composed of a screw, jack, displacement sensor, shim, etc., as shown in Figure 6. The horizontal loading device was tested by applying a horizontal load through a jack and transferring the horizontal load through a screw and a wire rope.

**2.4. Soil Collection from Undisturbed Soil.** Since one of the most important features of this test was the undisturbed soil model test, the indicators of soil in the soil collection site needed to conform to the test requirements. At the same time, the soil collection method needed to be more convenient and quicker to perform. As shown in Figure 8, soil collection involved eight steps [10], namely, leveling site, placing soil collector, pressing soil collector in soil, digging out soil collector, cleaning soil collector, packaging soil collector, transporting soil collector, and storing test specimens.

**2.5. Experimental Process.** After the sealed specimens from the site were brought to the laboratory, the following steps were taken: removing the side plate of soil collector, repairing the soil on the surface of the specimen, burying the model pile, drying the surface moisture, and installing the tempered glass, as shown in Figures 9–13.

In order to simulate the actual piles, a horizontal load should be applied when the pile was subjected to a vertical load (below its limiting value). The loading device developed during this study was utilized to apply the required loading scheme (the loading device and loading scheme have been applied for the national patent of the invention). The loading was divided into four steps [10], namely, adjusting the location of the soil collector, installing the vertical loading device, installing the horizontal loading device, and conducting the loading process.

### 3. Analysis of Test Results

The samples of the soil ring cutter used in the four groups of tests were taken to the laboratory. Since the samples of the

four groups were all undisturbed soil, which originated from the same site and had the same depth, the baseline parameters such as internal friction angle, moisture content, and density were basically the same between the site and the test.

**3.1. Analysis of the Failure Process of Soil.** During the test, a digital camera was used to record the failure process of soil around piles. The interaction of soil around piles was analyzed according to the data of displacement load and the pictures in the experimental process.

The horizontal load was applied to the pile top, and pictures were taken to record every 2 mm displacement at the pile top. Taking the flexible pile R3 with a distance of 40 mm from load-bearing plate to the pile top as an example, the failure process of soil around the pile is described through pictures, as shown in Figure 14.

Figure 14(a) shows the situation of applying a vertical load to the pile top. Figures 14(b)–14(h) show the situation of the pile top subjected to horizontal load. Once the vertical load was applied, small cracks were formed on the plate and the soil on the plate. The watermarking phenomenon appeared in the lower part of the load-bearing plate, which was due to the compression of soil by the vertical load on the load-bearing plate. When the horizontal load was applied to the pile top from the left-hand side, the pile top leaned toward the right. With an increase in the horizontal load, the watermark was gradually formed in the upper right and the lower left corners of the load-bearing plate, which was attributed to the compression of soil caused by the horizontal load on the bearing plate. As shown in Figures 14(b)–14(g), the upper part of the bearing plate was bent and inclined, which indicated that the bearing plate rotated along a certain point. The pile under the plate was inclined slightly, and the soil around the right pile was compressed. According to Figure 14(h), the cracking of soil around the pile in the upper part of the bearing plate was due to the fact that the horizontal tension generated by the pile on the soil around the pile was greater than the cohesive force of the soil around the pile itself, and the soil around the pile was destroyed at last.

In conclusion, the general trend of soil failure around the piles was as follows: with an increase in the horizontal load, the pile body on the right-hand side of the upper load-bearing plate exerted pressure on the soil around the pile, with the load-bearing plate rotating along a certain point. The soil around the pile was not disturbed beyond a relatively small depth at the lower part of the load-bearing plate. Because the compression produced by the pile body on the soil around the pile was greater than the cohesive force of the soil around the pile itself, the soil around the piles cracked and failed.

**3.2. Comparison of Failure States of Soil around Piles.** Comparisons were mainly made on the differences of failure states of soil around piles of G3 and R3, and G4 and R4. Under the action of load on the pile top and at the displacement of about 14 mm, different failure states appeared for different load-bearing dics. During the test, a

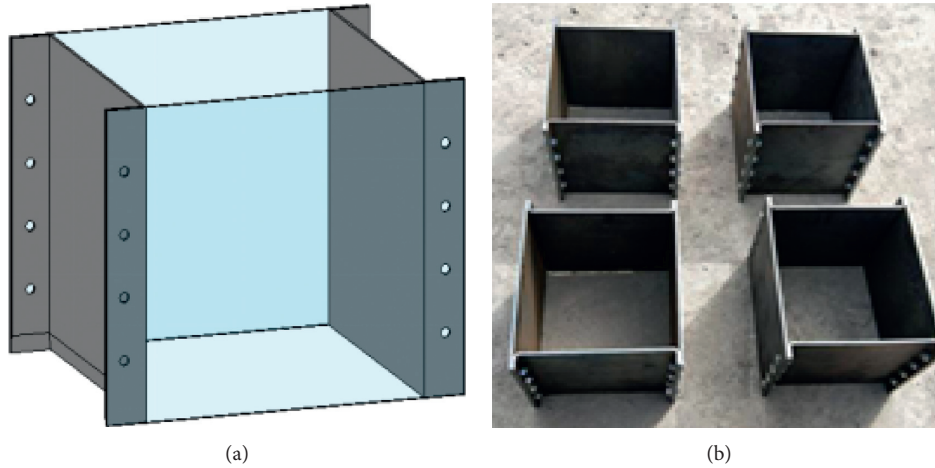


FIGURE 4: Soil collector. (a) Model for soil collector. (b) Actual picture for soil collector.



FIGURE 5: Multifunction test rig.



FIGURE 7: Horizontal loading device.



FIGURE 6: Vertical loading device.

displacement sensor was used to record displacement, and the failure state of soil around the pile was recorded by a camera. After the test, the collation results were compared

and analyzed. Figure 15 shows comparisons of the failure states of soil around different test piles.

As shown in Figure 15, the failure modes of soil around the four model piles were basically similar. In all cases, the soil on the upper part of the load-bearing plate and on the right side of the pile body was extruded, and the soil on the upper part of the load-bearing plate on the left side of the pile body was pulled. This was because the right side of the load-bearing plate played a role. When the horizontal load was applied to the model pile, the pile had an extrusion effect on the upper part of the right bearing plate, while it had a pulling effect on the lower part of the left bearing plate:

- (1) According to the comparisons of the soil failure states around G3 and R3, when the horizontal displacement on the top of both model piles was 14 mm, the degree of cracking of soil mass around the pile was different. G3 mainly showed rigid body rotation, with the whole pile body rotating along a certain



FIGURE 8: Collecting undisturbed soil at the site and making arrangements. (a) Leveling of soil collection. (b) Placing soil collector. (c) Pressing soil collector in soil. (d) Digging out soil collector. (e) Cleaning soil collector. (f) Packaging soil collector with plastic film. (g) Transporting soil collector. (h) Saving test specimens.



FIGURE 9: Removing the side plate of the soil collector.



FIGURE 10: Repairing the soil on the surface.

point on the load-bearing plate, and the upper soil on the right side of the load-bearing plate being subjected to compression. The upper part of the R3 pile



FIGURE 11: Burying a pile.

had local bending, while the part under the load-bearing plate remained unchanged for most of the loading range. Meanwhile, the soil around the lower part of the pile did not show obvious deformation, as shown in Figure 15(c).

- (2) As shown in Figures 15(e) and 15(h) (they are the failure states of soil around G4 and R4, respectively), it can be seen that the cracks become much smaller. In particular, for the flexible model pile R4, the upper part of the pile body underwent pure bending deformation, while the soil on the right was subjected to compression. The load-bearing plate played an insignificant role in the resisting bending moment. The pile G4 experienced a rigid body rotation.
- (3) A comparison of the rigid model piles G3 and G4 shows that both of them underwent rigid body rotation, but the displacement of the respective pile top



FIGURE 12: Drying the surface water.



FIGURE 13: Installing tempered glass.

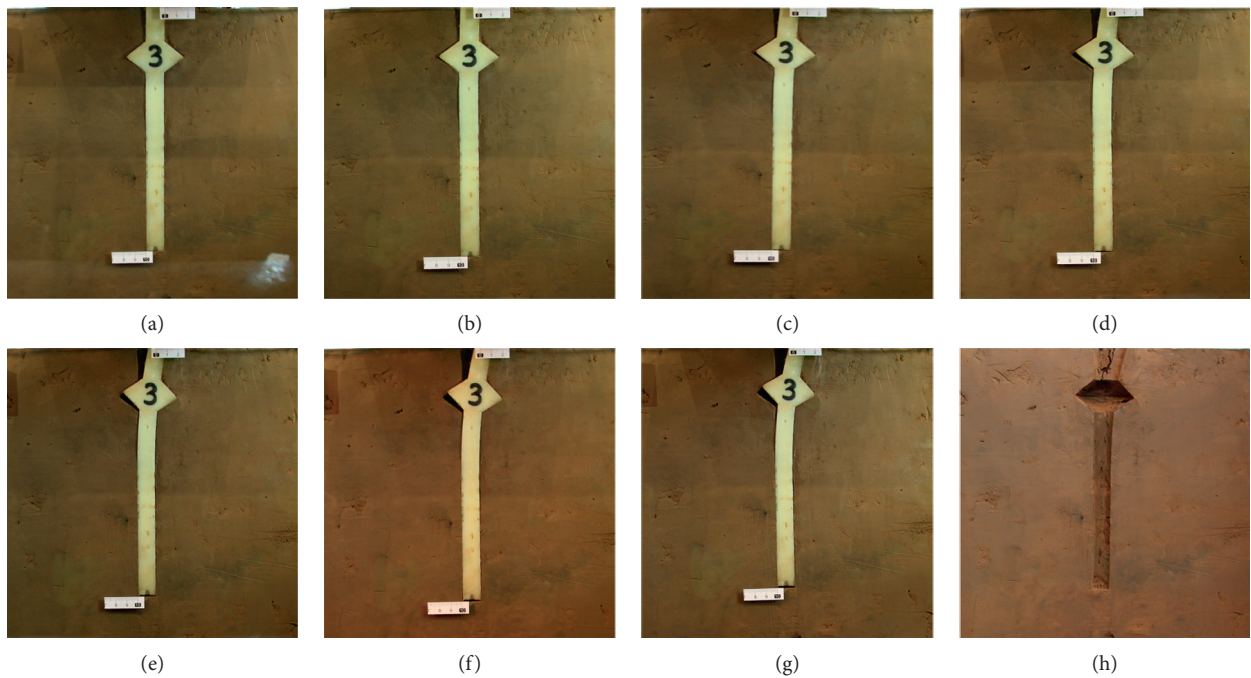


FIGURE 14: Pile and soil failure process for R3 pile.

was different. As shown in Figures 15(b) (G3) and 15(f) (G4), it can be clearly seen that the cracks formed on the soil around G3 were significantly

larger than those around G4. For the rigid concrete expanded pile, the distance from the bearing plate position to the pile top affected its horizontal bearing

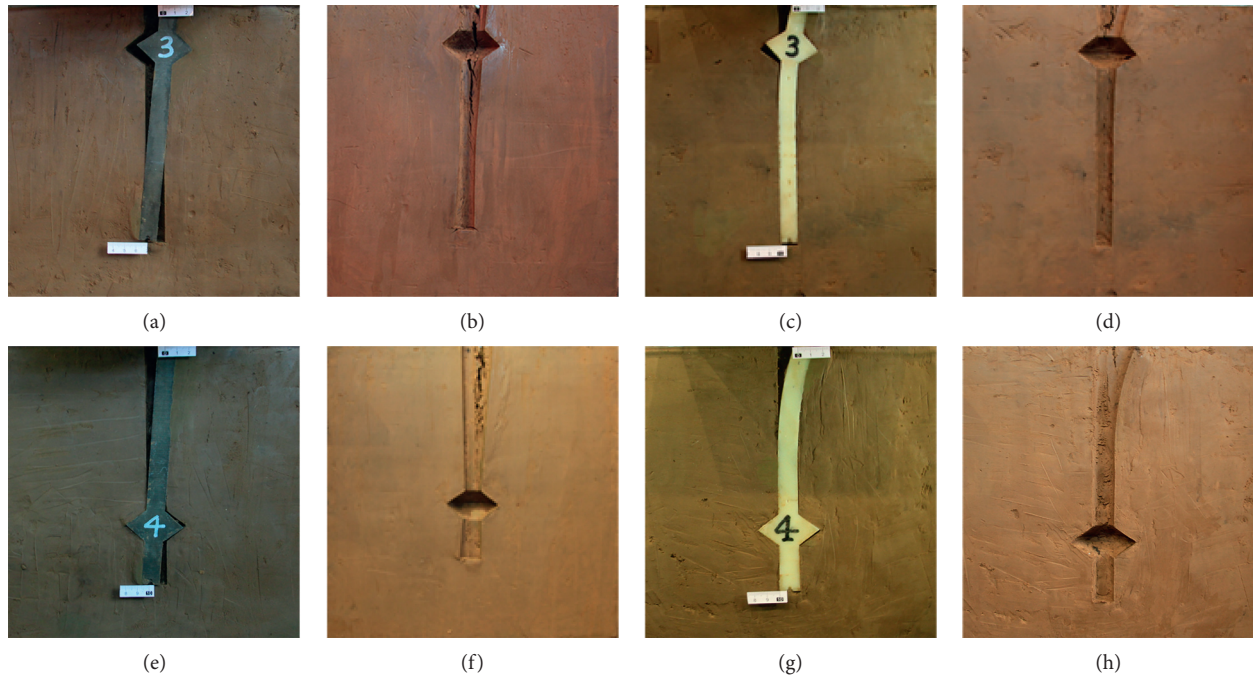


FIGURE 15: Comparison of soil failure state around different piles.

capacity: the shorter the distance between the location of the load-bearing plate and the pile top, the higher the horizontal load-bearing capacity, and the better the pile performance.

- (4) As shown in Figures 15(c) and 15(g), flexible model files R3 and R4 both exhibited pile bending. The load-bearing plate for R3 rotated along a certain point, while that for R4 was placed in the lower part and experienced no rotation at the end of the plate. Under the action of horizontal load, the load-bearing plate for flexible model pile R4 played an insignificant role.

**3.3. Analysis of Displacement-Load Data.** In order to make a detailed analysis of the horizontal load-bearing capacity of the concrete expanded pile, data on displacement and load were collected during the tests and were plotted as shown in Figure 16.

From the load-displacement curves in Figure 16, it can be seen clearly that the four curves roughly had a similar variation trend: with an increase in displacement, the horizontal load on the pile top also increased. At the initial stage of loading, the curves were relatively steep because the load-bearing plate became gradually effective with an increase in horizontal load. At the later stage of loading, the curves were less steep because the soil around piles failed with an increase in horizontal load. The change in the slope of the curve was most obvious for R3 pile. This indicated that the soil around the load-bearing plate pile had entered a failure state, causing the effect of the load-bearing plate to decrease gradually. For rigid concrete expanded pile, the distance between the location of the load-bearing plate and the pile top affected the horizontal bearing capacity of the

concrete expanded pile. Furthermore, the shorter the distance between the location of the load-bearing plate and the pile top, the greater the horizontal bearing capacity, and the better the pile performance. For a given horizontal displacement at the top of the model piles and for a relatively shorter distance between the location of load-bearing plate and the pile top, the rigid concrete expanded pile had stronger anti-overturning bearing capacity compared to the flexible pile. However, not much difference was observed between the horizontal bearing capacity of the rigid pile and the flexible pile when the distance between the bearing plate position and the pile top was relatively large.

#### 4. Finite Element Simulation Analysis on Rigid Piles and Flexible Piles

Finite element software ANSYS was used to simulate the influence of horizontal bearing capacity of different types of concrete expanded piles. The rigidity/flexibility of the expanded pile and the location of the load-bearing plate were important factors affecting the interaction between piles and soil, and the interaction state of piles and their failure were directly related to the bearing capacity of an individual pile.

**4.1. Finite Element Analysis Model.** In view of the limitations of boundary conditions, the domain of soil around the expanded pile should not be too small. When the simulation model was established, soil mass was selected to be a semicylindrical body with a diameter of 12.0 m and a height of 10.8 m. Three groups of rigid and flexible piles with the bearing plates at the same location were designed for comparison, and three representative locations from the load-bearing plate to the pile top were selected as research

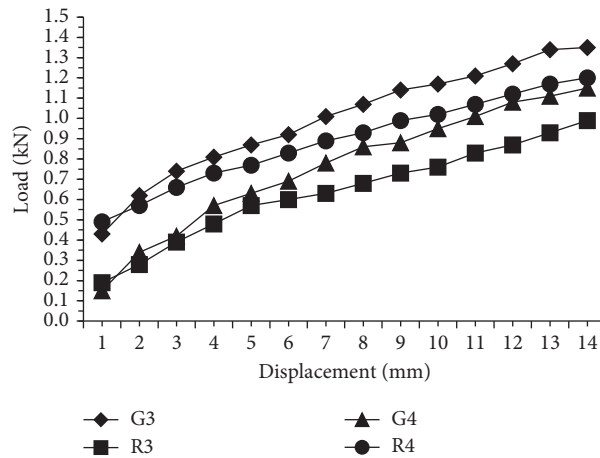


FIGURE 16: Displacement-load curves of the pile specimens.

objects, with the distance between the load-bearing plate and pile top being 1200 mm, 2400 mm, and 4800 mm, respectively. The corresponding designations of rigid concrete expanded piles were GM1, GM2, and GM3, and those of flexible concrete expanded piles were RM1, RM2, and RM3. Specific model parameters for piles were pile length  $L = 6800$  (mm), pile diameter  $d = 500$  (mm), plate diameter  $D = 1500$  (mm), plate height  $H = 800$  (mm), plate slope angle  $\alpha = 39$ , overhanging length  $R = 500$  (mm), and the distance between the plate and pile top  $L_1 = 1200$  (mm).

As shown in Table 1, concrete *G* was taken as the design parameter for rigid concrete expanded pile, Concrete *R* was taken as that for flexible concrete expanded pile, and silty clay was selected as soil mass. Specific parameters of materials were derived accordingly.

Soil was taken as an ideal elastomer and a linear elastomer material was used for the pile body. Horizontal load and vertical load were applied simultaneously. To make its failure mode similar to that found in actual sites, a 1 mm interval was designed between the load-bearing plate and the surrounding soil to ensure the interaction effect. SOLID65 solid element was used for concrete expanded pile, and the SOLID45 solid element was used for soil. When the pile surface came into contact with the soil interaction surface, the surface-surface contact pair was activated in the model [11, 12].

**4.2. Displacement Nephogram Analysis.** A fixed value of horizontal force (100 kN) was applied to three groups of rigid and flexible concrete expanded piles to obtain the displacement nephogram of pile-soil interaction in the *X* direction. The nephogram for the three groups of the expanded pile at different plate locations was analyzed as shown in Figure 17.

According to the comparison and analysis of displacement nephogram of rigid and flexible piles, as shown in Figure 17, the pile-soil interactions until the applied load of 100 kN were basically similar. All piles caused extrusion of soil on the upper right-hand side. With an increase in load, the compression effect of soil around the piles became

stronger, and the deformation of soil on the right side of piles was increased.

A careful observation of the action forms of the three groups of nephogram suggested that different displacements were generated at each pile top of the concrete expanded pile, which was caused by the different distances between the load-bearing plate and the pile top. Certainly, the failure states of soil around the piles were also largely different.

The maximum horizontal displacement appeared on the top of the piles. When the load applied to the top of the piles reached 100 kN, the horizontal displacement at the top of the model piles was 10.478 mm, 12.309 mm, and 13.805 mm, respectively, for GM1, GM2, and GM3, and 22.820 mm, 25.519 mm, and 28.484 mm, respectively, for RM1, RM2, and RM3. This indicated that the location of the load-bearing plate markedly influenced the resistance to horizontal force for rigid piles and flexible piles. The shorter the distance between the load-bearing plate and the pile top, the higher the anti-overturning bearing capacity, and the smaller the produced displacement for a given horizontal load.

When the location for the load-bearing expanded plate for piles was set to be fixed, the effect produced by rigid piles markedly differed from that by flexible piles. The comparisons of GM1 and RM1, GM2 and RM2, and GM3 and RM3 pairs in Figure 17 indicated that the greater the stiffness of expanded pile, the stronger the capacity of pile-soil interaction to resist the horizontal load. Moreover, the smaller the generated horizontal displacement, the better the pile performance.

**4.3. Displacement-Load Curves for the Models.** The data on displacement and load of three groups of expanded piles in *X* direction were collected, and the displacement-load curves at the pile top of the three groups of models were plotted as shown in Figure 18.

Based on the trend of curves in Figure 18 and the analysis of displacement-load curves for the pile top of rigid and flexible concrete expanded plate pile models, the following conclusions can be obtained:

TABLE 1: Parameters of the pile and soil materials for numerical modeling.

Material	Density ( $t/mm^3$ )	Elasticity modulus (MPa)	Poisson's ratio	Cohesion (MPa)	Friction angle ( $^\circ$ )	Dilation angle ( $^\circ$ )	Pile-soil friction coefficient
Concrete <i>G</i>	$2.5e-9$	$3e4$	0.2	—	—	—	
Concrete <i>R</i>	$2.5e-9$	$1e4$	0.2	—	—	—	0.4
Clay	$1.8e-9$	25	0.3	0.0174	18.29	18.29	

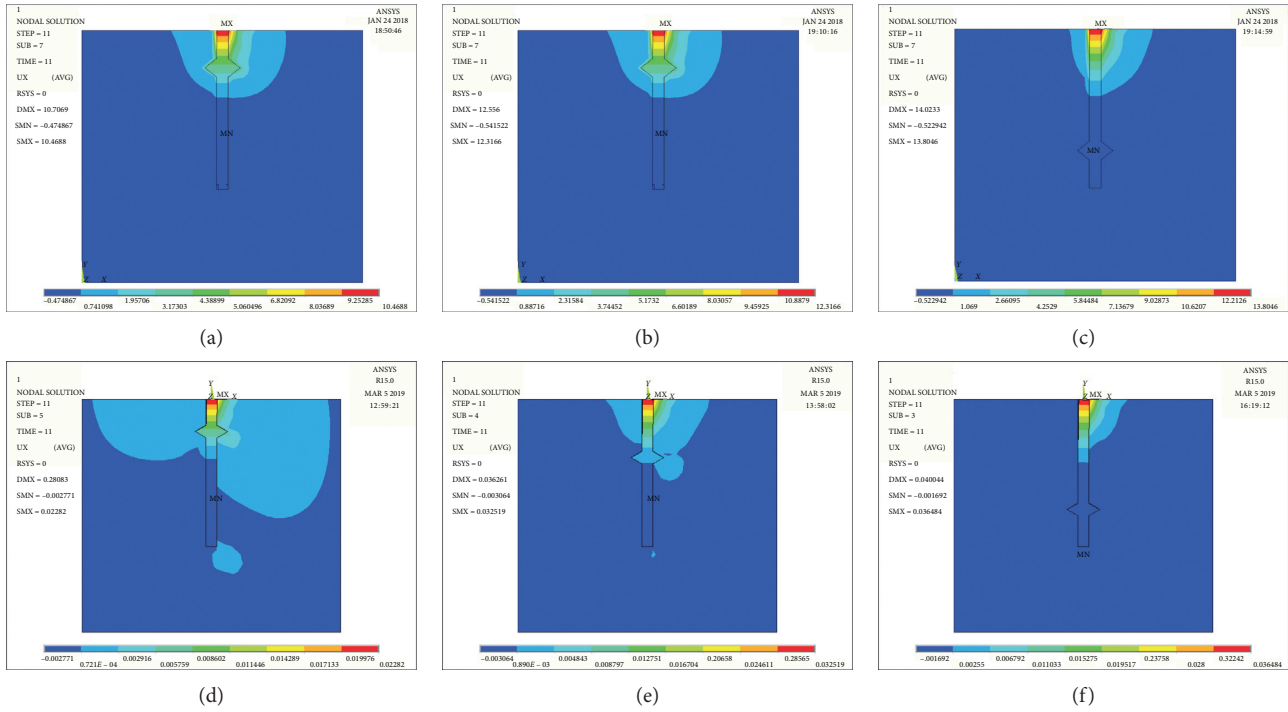


FIGURE 17: Displacement nephogram of rigid and flexible piles. (a) GM1 displacement nephogram. (b) GM2 displacement nephogram. (c) GM3 displacement nephogram. (d) RM1 displacement nephogram. (e) RM2 displacement nephogram. (f) RM3 displacement nephogram.

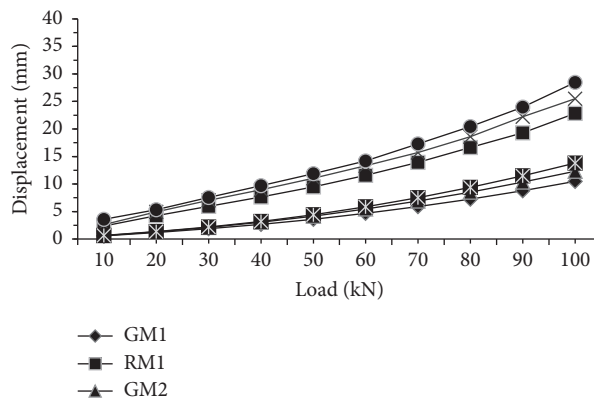


FIGURE 18: Simulated displacement-load curves of rigid and flexible piles.

(1) For a given horizontal load at the top of the concrete expanded piles, the horizontal displacement at the pile top of RM3 was the greatest, while that of GM1 was the smallest. When the horizontal displacements at the pile top were the same, the GM1 model had the

highest bearing capacity among the concrete expanded piles, indicating that it was the first to reach the ultimate state of bearing capacity. RM3 model had the lowest bearing capacity among the concrete expanded piles, indicating that it was the last to reach

the ultimate state of bearing capacity. Comparison of load-displacement curves for the pairs GM1 and RM1, GM2 and RM2, and GM3 and RM3 revealed that there were large differences in the displacements generated by rigid and flexible concrete expanded piles even if the locations of the load-bearing plates were identical. The greater the rigidity of the concrete expanded pile, the smaller the displacement generated, and the higher the anti-overturning bearing capacity. This indicated that the rigidity of concrete expanded piles was an important factor influencing the horizontal bearing capacity.

- (2) Detailed analysis of the load-displacement curves revealed that, at the initial stage of loading (when the load was smaller than 30 kN), the load-displacement curves for rigid concrete expanded piles GM1, GM2, and GM3 were basically identical. At this stage, the displacement of the pile top was relatively smaller, the load-bearing plate had no significant rotation, and the load-bearing plate did not produce a significant moment of resistance, indicating that the special advantages of the expanded pile were not materialized yet. When the load was greater than 30 kN, displacements of the pile top corresponding to different plate locations showed significant differences. This indicated that only after the displacement at the pile top reached a certain value, the load-bearing plate rotated, and the advantages of the expanded pile were fully realized. For a given load, the shorter the distance between the location of the load-bearing plate and the pile top, the smaller the displacement at the pile top.
- (3) Through the comparison of displacement-load curves for different expanded plate pile models, it can be seen that the trend of displacement-load curves of pile top in each model was nearly identical; that is, the horizontal displacement at the pile top of the concrete expanded piles gradually increased with an increase in horizontal load. Besides, the curvature of all displacement-load curves was greater. In particular, flexible concrete expanded piles RM1, RM2, and RM3 had steep curves, indicating that they all approached the ultimate state of bearing capacity relatively sooner. As the load continued to increase, the displacement nephogram in the X direction and the displacement-load curves showed that when the distance between the load-bearing plate and the pile top was 1200 mm and 2400 mm, respectively, the load-bearing plate played a greater role, and it also had a larger influence on the horizontal bearing capacity of the expanded pile. However, when the distance between the load-bearing plate and the pile top was 4800 mm, the load-bearing plate played an insignificant role and also had little influence on the horizontal anti-overturning bearing capacity of the expanded pile.

**4.4. Shear Stress Analysis of Rigid and Flexible Piles.** In three groups of piles, uniform points were selected on the whole pile and soil contact surface, and the shear stress values at the

selected nodes in the XY plane were summarized for a given horizontal load. As shown in Figure 19, curves were plotted according to the shear stress values of each point on the right side of the pile body.

*Note.* In Figure 19, the horizontal coordinate denoted the pile body node, and the vertical coordinate denoted the shear stress corresponding to the pile body node. The upward projections on the curves denoted the locations of the upper nodes on the load-bearing plate of the model piles, and the downward projections on the curves denoted the locations of the lower nodes. The highest point on the curves represented the upper inflection point of the expanded plate and the lowest point on the curves represented the lower inflection point of the expanded plate. The location between the highest point and the lowest point on the curves denoted the endpoint of the load-bearing plate.

Based on the analysis of Figure 19, the following findings can be obtained:

- (1) Change in shear stress of nodes on the rigid and flexible model piles along the pile axis reveals that, under the action of horizontal tension, the trend of the change in shear stress of rigid and flexible model piles was similar, and the shear stress values of the model piles showed abrupt changes at the upper and lower inflection points of the load-bearing expanded plates. The maximum shear stress occurred at the location of the load-bearing plate; the shear stress of the upper and lower parts of the expanded plate varied slightly along the pile body, and the shear stress of the pile body at the level of the load-bearing plate was significantly greater compared to the upper and lower parts of the pile body.
- (2) The maximum shear stress value in the XY plane was 2.88 MPa for the GM1 pile and 0.59 MPa for the GM3 pile, thus showing significant differences. The location of the load-bearing plate largely affected the change in shear stress value of the load-bearing plate. For a given rigidity, the shorter the distance between the location of the load-bearing plate and the pile top, the greater the shear stress of the pile body. This indicated that the shorter the distance between the load-bearing plate and the pile top, the more effective the pile in resisting the horizontal load.
- (3) Comparison of the pairs GM1 and RM1, GM2 and RM2, and GM3 and RM3 on shear stress curves of model pile body indicated that the maximum shear stress value of rigid piles was much greater compared to the flexible model piles when load-bearing plates were placed at a certain location. Therefore, the resistance to horizontal load was improved when the rigidity of the concrete expanded pile was relatively large.

Irrespective of the pile type as rigid or flexible, when the pile top was closer (1200 mm or 2400 mm) to the load-bearing plate, the force applied by the plate end to the surrounding soil was transmitted well, and the pile could bear a relatively large horizontal load. However, the distance between the location of the plate and the pile top should be

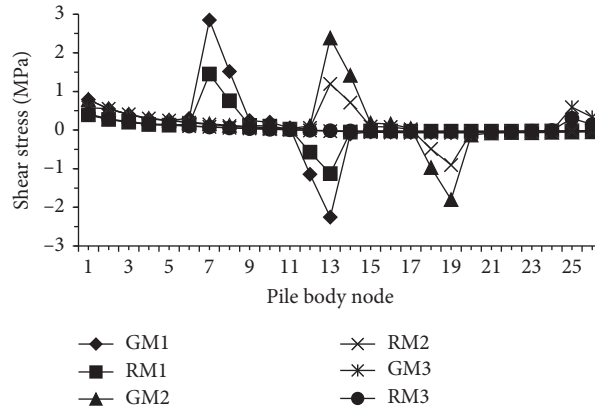


FIGURE 19: Diagram of shear stress curve of the pile body.

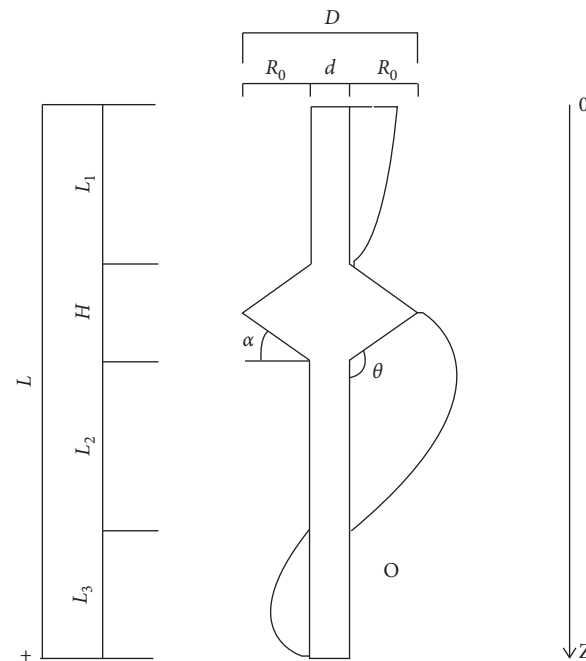


FIGURE 20: Stress mode of soil around a rigid expanded pile.

controlled within a reasonable range; otherwise, the pile would not be able to resist the overturning bending moment.

Based on the analysis of the displacement and stress results, it was concluded that the rigidity of the pile body influenced the horizontal bearing capacity of the expanded pile. When the load-bearing plate was placed at a given location, the greater the rigidity of the pile body, the stronger the anti-overturning bearing capacity of the expanded pile.

### 5. Calculation Model of the Horizontal Ultimate Bearing Capacity for Rigid and Flexible Expanded Piles

Failure modes of soil around rigid and flexible concrete expanded piles were determined by systematically exploring the failure states of the rigid and flexible concrete expanded

piles under the action of horizontal load [13, 14]. Under the action of a horizontal load, the stress mode of soil around rigid piles is shown in Figure 20, and that around flexible piles is shown in Figure 21.

According to the failure modes of soil around rigid piles and in combination with slipping-line theory [3, 4], the calculation model for anti-overturning ultimate load-bearing capacity of a single rigid concrete expanded pile is proposed as follows:

$$F = F_{ep} + F_{sp}, \quad F \leq F_p, \quad (1)$$

where  $F_{ep} = \pi((D + d)/4)c \cot \varphi R_0 (e^{2\theta \tan \varphi} - 1)$ ,  $F_p = ((3EI \omega)/(L - L_3)^3)$ , and  $F_{sp} = F_1 + F_2 = \int_0^{L_1} mY_0 b_0 dz + \int_{L-L_3}^L mY_0 b_0 dz$ .

According to the failure modes of soil around rigid piles and in combination with slipping-line theory, the

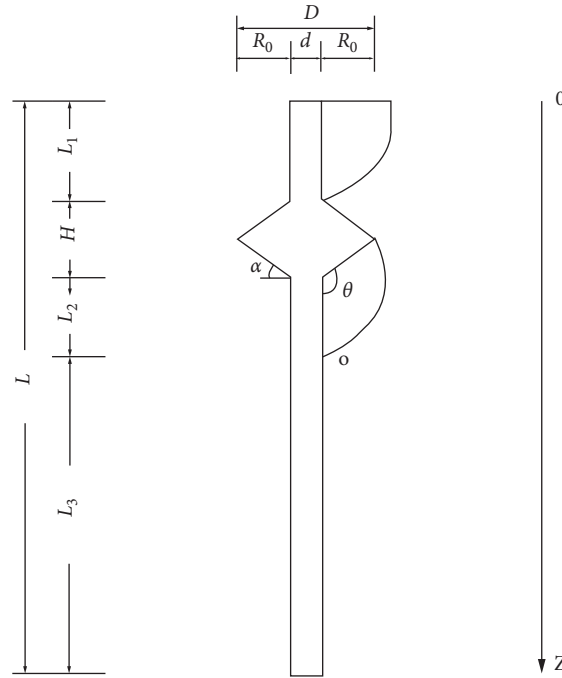


FIGURE 21: Stress mode of soil around a flexible expanded pile.

calculation model for the horizontal ultimate bearing capacity of a single flexible pile is proposed as follows:

$$F = F_{ep} + F_{sp}, \quad F \leq F_p, \quad (2)$$

where  $F_{ep} = \pi((D + d)/4)c \cot \phi R_0 (e^{2\theta \tan \phi} - 1)$ ,  $F_p = (3EI \omega / (L - L_3)^3)$ , and  $F_{sp} = F_1 + F_2 = \int_0^{L_1} mY_0 b_0 dz + \int_{L_1}^{L-L_3} mY_0 b_0 dz$ , where ep is the end of the plate; sp is the side of the pile; p is the pile body;  $c$  is the cohesion of soil around piles;  $d$  and  $D$  are the diameter of pile body and bearing plate, respectively;  $\phi$  is the internal friction angle of soil around piles;  $\theta$  is the angle between the lower surface of the plate and the vertical direction;  $F_1$  is the  $L_1$  region's bearing capacity;  $F_2$  is the  $L_2$  region's bearing capacity;  $F_n$  is the ultimate bearing capacity of soil corresponding to a unit width of the plate;  $L$  is the full length of the expanded pile. Moreover,  $m$  is the proportional coefficient for resistance coefficient of soil varying with depth;  $L_1$  is the length of the vertical pile body on the plate;  $L_2$  is the length of the vertical pile body below the slipping line.  $E$  is the modulus of elasticity of materials;  $I$  is the moment of inertia of piles;  $\omega$  is the displacement of the pile top under the horizontal load.

The calculation models for the anti-overturning bearing capacity of rigid and flexible concrete expanded piles were summarized. In summary, the calculation models for rigid and flexible piles were different for the side resistance and nearly the same for the underplate resistance.

## 6. Conclusions

This paper investigated the horizontal load-bearing capacity of rigid and flexible concrete expanding piles by performing experimental and numerical studies. Through small-scale half-section model test and ANSYS finite element simulation

analysis, the following conclusions were drawn on the failure states and bearing mechanism of soil around rigid and flexible concrete expanded piles when subjected to a horizontal load:

- (1) When the distance between the location of the load-bearing plate and the pile top was relatively shorter, rigid piles experienced rigid body rotation while flexible piles experienced local bending at the upper part. This observation remained unchanged in a large-scale range under the load-bearing plate. Meanwhile, the soil around the lower parts of the piles exhibited no significant deformation. For a given location of the load-bearing plate, the greater the rigidity of the concrete expanded pile, the higher the anti-overturning bearing capacity of the expanded pile. For the distance between the location of the load-bearing plate and the pile top of up to 1200 mm, rigid model piles still exhibited rigid body rotation, the upper part of the flexible piles still showed local bending, and the load-bearing plate did not rotate. The load-bearing plate played an insignificant role in resisting the bending moment. This demonstrated that the relative location of the load-bearing plate is an important factor affecting the horizontal bearing capacity.
- (2) For a given location of the load-bearing plate, displacements at the pile top of the rigid and flexible piles were markedly different. The greater the rigidity, the smaller the displacement at the pile top and the higher the anti-overturning bearing capacity. Irrespective of the pile type as rigid or flexible, when the pile top was closer (1200 mm or 2400 mm) to the load-bearing expanded plate, the load applied by the

plate end to the surrounding soil was transmitted well, and hence, the pile could bear a relatively large horizontal load. However, the distance between the location of the plate and the pile top should be controlled within a reasonable range; otherwise, the increased resistance to bending moment cannot be realized.

- (3) A comparison of the small-scale semisection model test and the ANSYS finite element simulation analysis revealed that the failure states of soil around piles were basically the same for rigid and flexible piles. The overall trends of the load-displacement curves of the pile top were similar both in the test and in the numerical simulation.
- (4) Since failure states of the rigid and flexible concrete expanded piles subjected to a horizontal load were markedly different, two separate calculation models were proposed for the anti-overturning bearing capacity of the rigid and flexible piles, respectively. These models provide a theoretical basis for the design and application of concrete expanded pile.

Concrete expanded pile mainly used in high-rise buildings, high-rise structures, offshore platforms, dams, high-speed rail foundation, underground space, and wind power equipment foundation. The application field of expanding pile under horizontal load was civil engineering, hydraulic power, electric power, etc. The advantages are high bearing capacity, small settlement, being suitable for complex soil layer, etc. The disadvantages are the need for special equipment to pile and the cost being slightly higher than that of the straight-hole pile. In this paper, the influence of horizontal force on the soil failure state of rigid and flexible concrete expanded piles was studied. The bearing capacity of the expanded pile under horizontal load was seen to be improved due to the expanded plate. Rigid pile and flexible pile were analyzed in detail. Further research should be performed on the influence of various parameters of flexible concrete expanded piles, such as the geometry and location of the load-bearing platform and the number of load-bearing plates on bearing capacity of the piles.

### Data Availability

The data used to support the findings of this study are included within the article.

### Conflicts of Interest

The authors declare no conflicts of interest.

### Acknowledgments

This work was financially supported by the National Natural Science Foundation of China (51678275).

### References

- [1] Z.X. Zhao, "Finite element analysis of extruded branch and disk pile under horizontal load, Taiyuan," Master thesis, Taiyuan University of Technology, Taiyuan, China, 2007.
- [2] F. M. Abdrabbo and A. Z. El Wakil, "Laterally loaded helical piles in sand," *Alexandria Engineering Journal*, vol. 6, no. 55, pp. 3239–3245, 2016.
- [3] Q. Li, M. He, and Y. Tan, "Experimental study on extruded branch plate supporting pile," *Geotechnical Mechanics*, vol. 9, no. 10, pp. 146–149, 2005.
- [4] G. Xiaoyuan, W. Jinchang, and Z. Xiangron, "Static load test and load transfer mechanism study of squeezed branch and plate pile in collapsible loess foundation," *Journal of Zhejiang University Science A*, vol. 8, no. 7, pp. 1110–1117, 2007.
- [5] Y. Li, Y. Wang, and X. Gao, "Finite element analysis of deformation behavior of squeezed branch pile group under horizontal load," *Journal of Henan University of Technology (Natural Science Edition)*, vol. 5, no. 2, pp. 234–238, 2008.
- [6] L. Zhao, L. Xiang, C. Lu, and S. Han, "Analysis of stress characteristics of squeezed branch pile group under horizontal load," *Industrial Building*, vol. 39, no. 10, pp. 52–56, 2009.
- [7] S. Kumar and S. Prakash, "Estimation of fundamental period for structures supported on pile foundations," *Geotechnical and Geological Engineering*, vol. 22, no. 3, pp. 375–389, 2004.
- [8] J. Z. Xing and J. Li, "The modeling method and the mesh division of the ANSYS," *China Water Transport (Academic)*, vol. 10, no. 9, pp. 116–118, 2006.
- [9] D. Jihui, C. Yanliang, W. Weiyu, Z. Tuo, and F. Junhui, "Experimental study of dynamic characteristics on composite foundation with CFG long pile and rammed cement-soil short pile," *Open Journal of Civil Engineering*, vol. 4, no. 9, pp. 1–12, 2014.
- [10] Y. Qian, J. Wang, R. Wang, and Z. Lian, "Research status and working mechanism of concrete expanded pile under horizontal load," *Shanxi Architecture*, vol. 42, no. 13, pp. 62–63, 2016.
- [11] Q. Yongmei, Z. Rongzheng, and W. Ruozhu, "Research on the calculating mode of the uplift bearing capacity of the concrete expanded-plates pile," *Architectural Engineering and New Materials*, vol. 2, no. 12, pp. 240–247, 2015.
- [12] D. Qian, C. Sun, and D. Wang, "Study on the interaction law between squeezed branch pile and soil," *Foundation Analysis and Design*, vol. 24, no. 6, pp. 218–225, 2004.
- [13] R. J. Finno and H. Chao, "Guided waves in embedded concrete piles," *Journal of Geo Technical and Geo Environmental Engineering*, vol. 131, no. 1, pp. 11–19, 2005.
- [14] Y. Qian and X. Xie, "The research on collapse state and stress performance of push-extend multi-under-reamed concrete pouring pile in the fine powder sand," *Energy Education Science and Technology (EESTA) Part A*, vol. 32, no. 4, pp. 2493–2498, 2014.